Automotive Science and Engineering

Journal Homepage: ase.iust.ac.ir

Effect of inlet flow condition on the thermal behavior of battery pack using a wavy cooling jacket

Ali Modarresi [1], Saman Samiezadeh[2], Ali Qasemian[3]*

[1] Ph. D student, School of Automotive Engineering, Iran University of Science and Technology

[2] M. Sc, School of Automotive Engineering, Iran University of Science and Technology

[3]* Ph.D., Assistant professor, School of Automotive Engineering, Iran University of Science and Technology

ARTICLE INFO	ABSTRACT
	In recent years, the automotive industry has experienced a dramatic mutation in the develop ment of electric vehicles. One of the most important aspects of this type of vehicle is its thermal management. Among the various parts of an electric vehicle that are subjected to thermal management, the battery is of particular importance. Battery cell temperatures may exceed the allowable range due to continuous and high-pressure operation and various weather conditions, and this, in addition to performance, severely affects battery life. Therefore, the appropriate cooling system is essential. In this research, the most common methods of battery cooling are investigated. First, three-dimensional thermal analysis on the battery is performed using the computational fluid dynamics method in transient and steady-state phases. Then, the effect of changing the cooling flow rate on the maximum temperature of the battery cell as well as the temperature difference of the cells in the battery pack is investigated. The effect of changing inlet coolant temperature change on battery cell temperature distribution is also investigated. The results show that by increasing the flow rate from 0.5 to 1.2 liter per minute, the maximum temperature in the battery pack and the temperature difference between the cells decrease to 44.4 and 2.51 ° C, respectively. Also, by changing the temperature of the inlet coolant from 15 to 30 ° C, the maximum temperature in the battery pack increases up to 42.2 ° C and the temperature difference is negligible.

1. Introduction

Today, the automobile industry is rapidly moving towards modern powertrain vehicles to reduce environmental issues [1, 2]. Currently, lithium-ion batteries are widely used in electric and hybrid vehicles. The reason for their widespread use is the high specific energy, power density, and lifetime with the low self-discharge rate [3-5]. The performance and efficiency of battery cells depend on how they manage their heat [6, 7]. The battery thermal management system must be designed so that the battery cells perform optimally with no

damage in hard-working conditions [8, 9]. In addition, as an essential factor, temperature affects various aspects of the lithium-ion battery, including thermal and electrochemical behaviors which can affect the vehicle's performance [10, 11]. The normal temperature of battery cells for optimal performance is 20 to 40 degrees Celsius [12, 13]. Likewise, a battery thermal management system with proper performance should reduce the temperature difference of battery cells in the battery module to less than 5 degrees Celsius [14, 15]. There are different approaches for battery

thermal management systems, which include: 1) air cooling and 2) liquid cooling. The air-cooled approach has attracted the attention of many researchers due to its simplicity and lightweight [16]. The liquid-cooling approach is more optimal than the air-cooled method due to better heat absorption.

Additionally, due to the low conductivity of air [17], a very high airflow rate is required to cool the battery cells adequately [18]. On the other hand, the liquid-cooling method gives a better result in terms of cooling than the air-cooling method due to its high thermal conductivity. Although cooling through water requires more complexity and cost [19, 20].

Researchers have carried out several works on battery thermal management systems using different methods including neural networks [21, 22], finite element model [23, 24], LUMPED method [25], partial differential equations method [26], and computational fluid dynamics [27-29]. Lin and his colleagues [30] have investigated the effect of using phase change materials using the computational fluid dynamics method as well as the experimental method. They concluded that the use of phase change materials significantly reduces the temperature of the battery during harsh operating conditions. They also concluded that the temperature uniformity in the module decreases with the increase in the discharge time and also the flow rate. Rao and his colleagues [31] have used a three-dimensional model using Ansys Fluent software for battery thermal modeling. In this research, they investigated the effect of changing the mass flow rate of water, the temperature of the phase change material, and its thermal conductivity on the thermal behavior of the battery. Results showed that the liquid volume ratio of the phase change material is strongly influenced by its temperature and thermal conductivity. Also, the results showed that increasing the channels reduces the maximum temperature of the battery as well as the temperature difference between the battery cells. Using experimental and numerical methods, Mir Mohammedi and his colleagues [32] investigated the effect of using different nanofluids on the cooling of the lithium-ion battery and the heating of the battery during discharge. The results showed that the temperature of the battery cells reached 350.31 K after 300 seconds with the use of water-alumina nanofluid at a rate of 5C. While using air fluid for cooling, the temperature of the complex increases by about 10 Kelvin. Also, the results showed that the battery discharge rate using water-gold nanofluid is lower than air and water as

well as other nanofluids. Wang [33] has investigated the effect of air cooling with forced displacement on the cylindrical battery pack with the help of numerical methods to design optimally for the battery pack. In another paper, Wang [34] presented an effective reciprocating air-cooling method to control battery temperature. Hugh and his colleagues [35] have designed small channels on the cold plate for cooling rectangular battery cells. They have investigated the effect of the ambient temperature, the number of channels, the flow direction, and the mass flow rate of the incoming fluid on the temperature distribution and the increase in battery temperature during battery discharge. They concluded that the maximum temperature of the battery decreases with the increase in the mass flow rate and the number of channels.

As seen in the literature review, despite various studies on the electric vehicle battery cooling system, no comprehensive research has been done on the heat transfer of lithium-ion battery cells with a cylindrical geometry with the help of fluid cooling. In this research, the three-dimensional analysis of the cooling of the battery pack in transient and steady states is discussed using ANSYS Fluent software. Then, the effect of c the volume flow rate on the maximum temperature of the battery pack and the temperature difference between the battery cells is investigated.

2. Approach

2.1. Geometry

A wavy liquid-cooling channel is used for the battery thermal management system with 2688 pieces of 21700 cylindrical Li-ion battery cells. The schematic of this system is shown in Figure 1. Channel depicted in Figure 2 is made of aluminum. It should be noted that the battery pack consists of 16 modules. Each module has two coolant passages. As the channels are identical and symmetrical, the simulation is performed for only one channel.
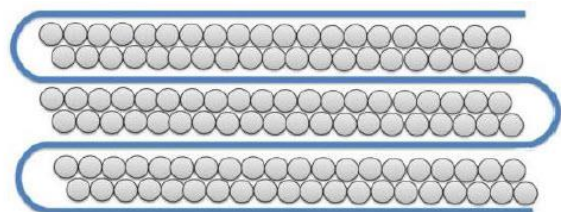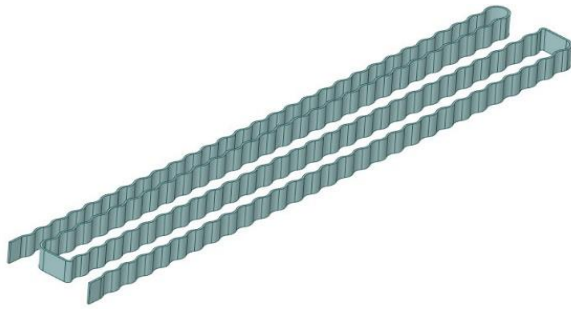

Figure 1: Schematic of cooling system

Figure 2: Cooling channel

The geometrical specification of the channel and battery cell is given in Table 1.

Table 5: The geometry specification of coolant passage and battery cells

Channel width (mm)	2
Channel height (mm)	30
Battery cell diamterer (mm)	21
Battery cell height (mm)	70
Number of cells in the module	168

2.2. Meshing

An unstructured mesh of polyhedron elements was generated using Fluent meshing. The main advantage of this meshing tool is producing high-quality meshes at a faster turnaround time compared to other tools. Moreover, this tool is more suitable for conformal and non-conformal interfaces for conjugate heat transfer models. The mesh includes two zones: a fluid zone for the coolant, and a solid zone for battery cells. The total number of mesh generated in this model is 4,525,747 which consists of 1,815, 470 elements for the solid domain and 2,710,277 for the fluid domain. Figures 3 and 4 illustrate the mesh of fluid and solid regions respectively. The minimum and maximum mesh sizes are 0.05 mm and 0.8 mm, respectively.
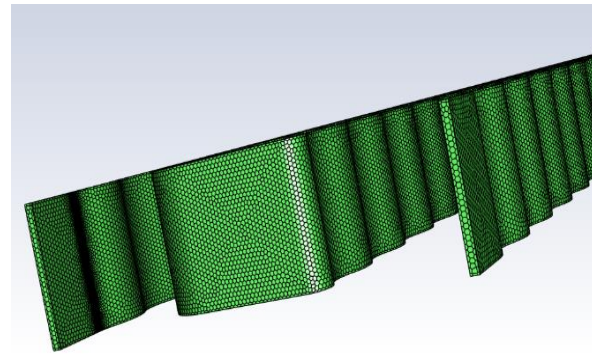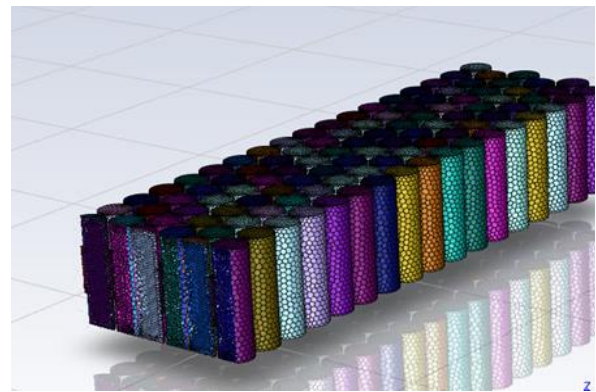

Figure 3: Coolant passage mesh

Figure 4: Solid region mesh

The Smooth transition method is utilized for generating the boundary layer meshes depicted in Figure 5. the k-ω model due to high accuracy is used for modeling turbulence. Note that the standard wall function is utilized near the wall.
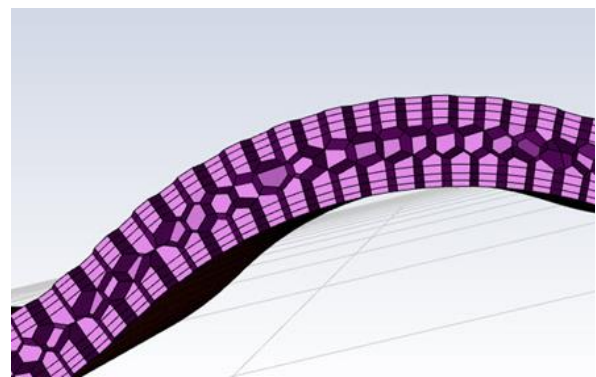

Figure 5: The boundary layer mesh

The quality of generated mesh in terms of skewness and orthogonal quality is given in Table 2. As seen, the maximum skewness for both regions is lower than 0.5 which represents the high-quality mesh.

Table 2: Quality of generated mesh

Part	Average skewness	Maximum skewness	Orthogonal quality
Cooling channel	213	0.295	423
Battery cells	201	0.307	424.5

2.3. Governing equations

The main governing equations of fluid flow including continuity, momentum, and energy are given by (1)-(5) respectively. The conjugated heat transfer method is used to determine the temperature distribution of coolant passage and battery cells.

$$\frac{\partial \rho}{\partial t} + \frac{\partial}{\partial x_i}(\rho u_i) = 0 \tag{1}$$

$$\frac{\partial}{\partial t}(\rho u_i) + \frac{\partial}{\partial x_j}(\rho u_i u_j) = -\frac{\partial P}{\partial x_i} + \frac{\partial \tau_{ij}}{\partial x_i} + \rho g_i + F_i \tag{2}$$

$$\tau_{ij} = \left[\mu \left(\frac{\partial u_i}{\partial x_j} + \frac{\partial u_j}{\partial x_i} \right) \right] - \frac{2}{3} \mu \frac{\partial u_1}{\partial x_1} \delta_{ij} \tag{3}$$

$$\rho \frac{Dh}{Dt} - \nabla . k\nabla T - \nabla . \left[\sum_j \gamma_j h_j \nabla m_j \right] - \mu \emptyset - \frac{DP}{Dt} - S$$
$$= 0 \tag{4}$$

$$\emptyset = \left[\frac{\partial u_i}{\partial x_j} + \frac{\partial u_j}{\partial x_i} - \frac{2}{3} \mu \frac{\partial u_1}{\partial x_1} \delta_{ij} \right] \frac{\partial u_j}{\partial x_i} \tag{5}$$

2.3. Governing equations

Ethylene glycol/water mixture (50%) is considered the coolant for the battery thermal management system. The physical and thermal characteristics of the coolant such as density, dynamic viscosity, thermal conductivity, and heat capacity at the temperature of 20°C are shown in Table 3.

Table 3: Properties of battery cooling fluid at 20 °C

Property	Value
Density ($\frac{kg}{m^3}$)	1079
Specific Heat ($\frac{j}{kg.K}$)	3472
Thermal Conductivity ($\frac{W}{m.K}$)	0.38
Dynamic Viscosity ($\frac{kg}{m.s}$)	0.41

Also, the thermal and physical properties of the battery cell at 30 °C are given in Table 4.

Table 4: battery properties at 30 °C [38]

Property	Value
Density ($\frac{kg}{m^3}$)	1605
Specific Heat ($\frac{j}{kg.K}$)	2615.7
Thermal Conductivity ($\frac{W}{m.K}$)	3
Internal resistance (mΩ)	25

2.4. Initial conditions

The initial temperature in steady state simulation for coolant and battery cell is considered to be 25°C and 30 °C respectively. The coolant flow rate for both steady and transient states is 1 Lit/min.

2.5. Boundary conditions

Velocity inlet and pressure outlet are considered boundary conditions at the inlet and outlet of the coolant passage. Also, It is needed to define the interface as a boundary between the solid and fluid regions. In the solid region, thermal losses due to the heat generated by battery cells should be calculated. This loss depends on current and internal resistance. The internal resistance of the battery cell is 25mΩ and the amount of current that flows through the battery pack in terms of time is given in Figure 6.
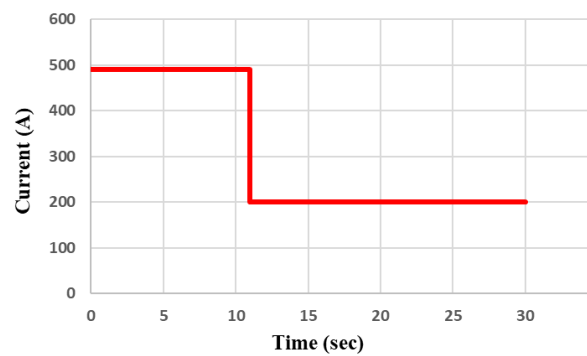

Figure 6: The amount of current in terms of time

As seen in Figure 6, the amount of current is 490amps for the first 11 seconds and then is reduced to 200amps which corresponds to the nominal current of electric components. The maximum current is calculated according to the maximum power consumed by electric

components at the battery pack voltage of 360V in the acceleration mode. The heat generated by a battery cell can be written as per:

$$P_{cell} = {R_{eq}I^2}/{n} \qquad (6)$$

Where R_{eq} , n and I are equivalent resistance, number of cells, and current. The configuration for the battery pack is parallel-serial connections which 96 cells are in series and 28 are in parallel. The amount of thermal losses during transient and steady states is given in Table 5.

Table 5: The battery cell thermal loss during transient and steady states

Operation state		Value (W)
Steady		1.27
Transient	11 sec ≤	7.65
	11 sec >	1.27

3. Results

In this section, the thermal and fluid flow results of numerical simulation are presented. Then the effects of volume flow rate and inlet temperature on the temperature distribution of the battery pack are investigated.

3.1. Grid independency

To demonstrate mesh independency, three additional meshes were generated and their results in terms of pressure drop at a flow rate of 1 lit/min are presented in Figure 7.
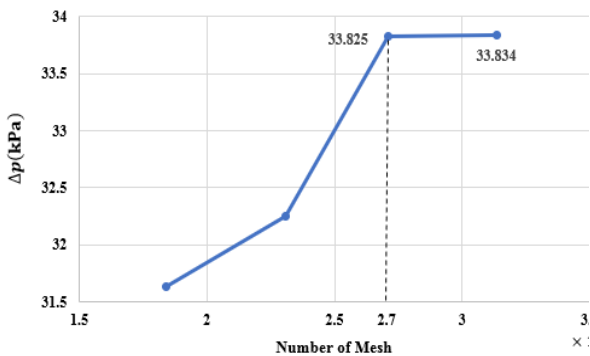

Figure 7: Mesh independency test

According to Figure 7, for the number of elements that is more than 2710277, the pressure drop difference is lower than 1%. Therefore, this grid number is used in this study.

3.2. Steady state

3.2.1. Pressure analysis

Figure 8 shows the pressure drop contour of the coolant passage at a volume flow rate of Lit/min.
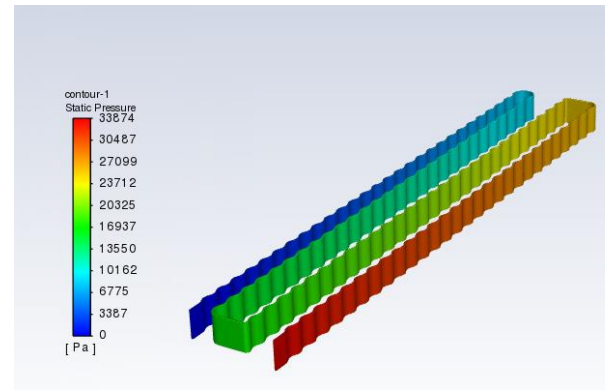

Figure 1: Pressure drop contour

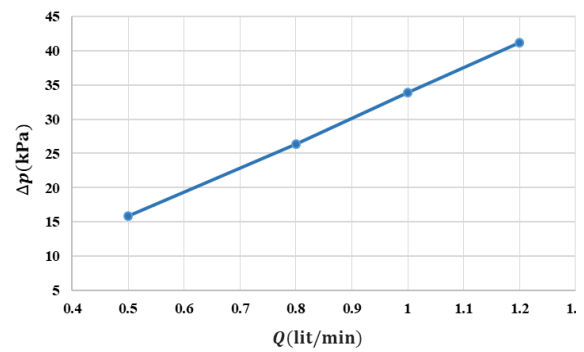The value of pressure loss between the inlet and outlet at different volume flow rates is demonstrated in Figure 9.

Figure 9: Pressure drop at different volumetric flow rates

Table 6 shows the pumping power at different flow rates.

Table 3: Properties of battery cooling fluid at 20 ℃

Volume flow rate (Lit/min)	Pumping power (W)
0.5	0.13
0.8	0.35
1	0.56
1.2	0.82

3.2.2. Temperature analysis

The temperature distribution of the battery pack, coolant passage, two adjacent cells, and one under

steady-state operation is illustrated in Figure 11. In this state, the volume flow rate and inlet coolant temperature are set to be 1 Lit/min and 25 °C.
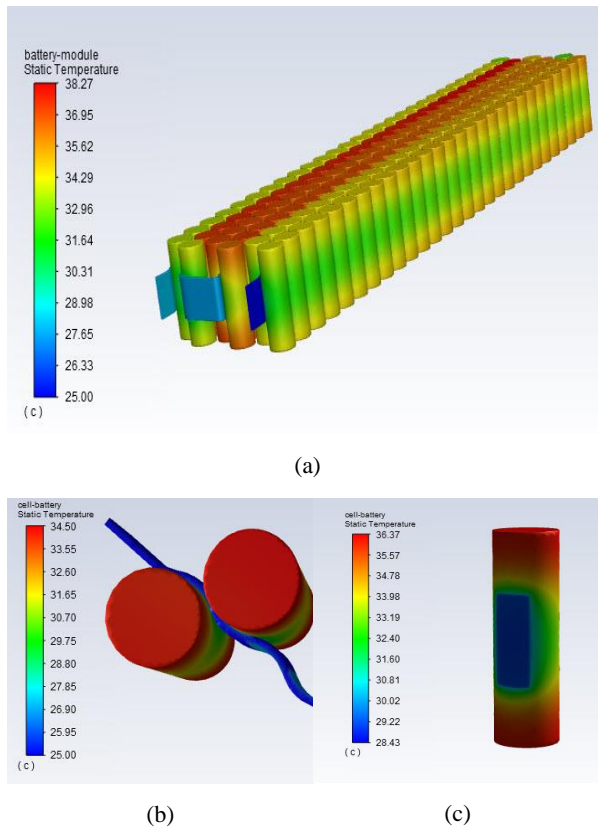

(a)

(b)   (c)

Figure 10: Temperature distribution in the steady state; a) battery module, b) two adjacent cells, c) battery cell

According to Figure 10, the maximum temperature in the battery pack reaches 27.38 °C. The average temperature difference of the battery cells is also 4.97 °C, which is lower than the permissible criteria (5 °C) for the temperature difference between battery cells (°C). The cell located at the end of the second row has the lowest temperature due to the highest contact with the coolant passage compared to other cells. The maximum and minimum average temperature of battery cells is 36.22 and 31.35 °C respectively.

3.3. Transient state

According to Newton's second law, in the acceleration mode, the driving force of the electric motor and the current required by the electric components will increase. At constant speed, the power produced by the electric motor is equal to the sum of the aerodynamic drag, and rolling resistance.

Acceleration mode is always accompanied by the maximum current and consequently heat losses. Therefore, considering the importance of the

acceleration period, the thermal analysis of the battery cells in the transient state is necessary. By considering the heat loss stated in sections 5-2, the coolant temperature and the average battery cells temperature during 30 seconds period at a volume flow rate of 1 Lit/min are shown in Figure 11.
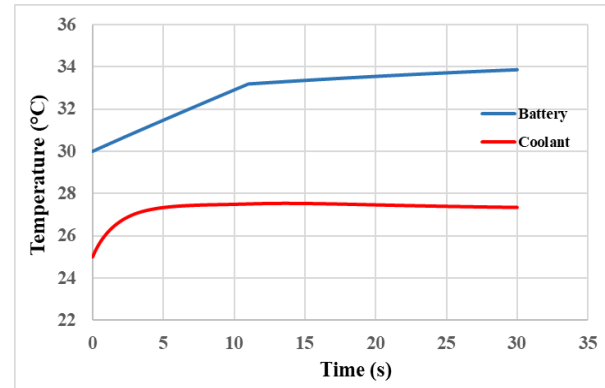

Figure 11: The average temperature of battery cells and coolant in the transient state

As seen in Figure 11, the average temperature of battery cells increases by 4 °C for 30 seconds. The coolant temperature reaches 27 °C. According to the above graph, the battery temperature slope decreases after 11 seconds. The reason for this is the reduction of heat dissipation of each battery cell from 7.65 to 1.27 W. Regarding the coolant temperature, at the beginning of the simulation, the temperature slope has an upward trend due to the higher heat produced by the battery cells compared to the cooling power. After 11 seconds, the slope of the line decreases due to the reduction of the heat generated by the battery cells. In other words, after this period, the cooling power becomes higher than the rate of energy produced by battery cells.

Figure 12 shows the temperature distribution of the battery pack, coolant passage, and one cell. According to the temperature contour of one cell, the part of the battery cell contacted to the cooling channel has a lower temperature compared to the upper and lower surfaces of the cell.
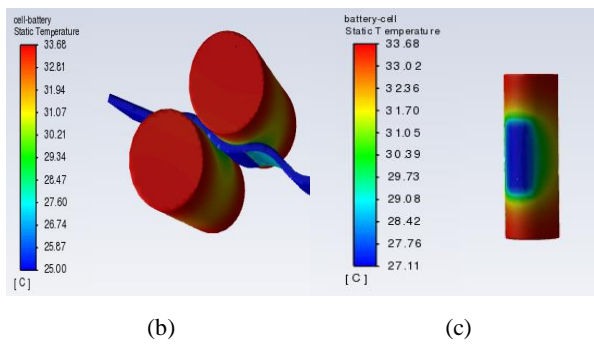

(a)

(b)   (c)
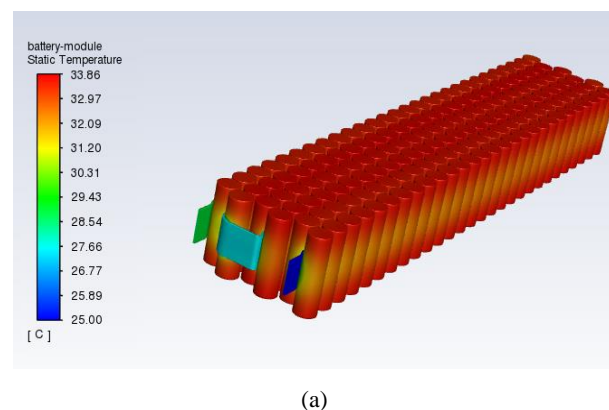
Figure 12: Temperature distribution in the steady state; a) battery module, b) two adjacent cells, c) battery cell

3.3. The effect of coolant flow rate and inlet coolant temperature

After finding the temperature distribution across the pack, the impact of parameters including volume flow rate and inlet coolant temperature was proposed. Figures 13 and 14 show the effect of coolant flow rate and coolant temperature at the inlet on the average temperature difference and maximum temperature within the pack.
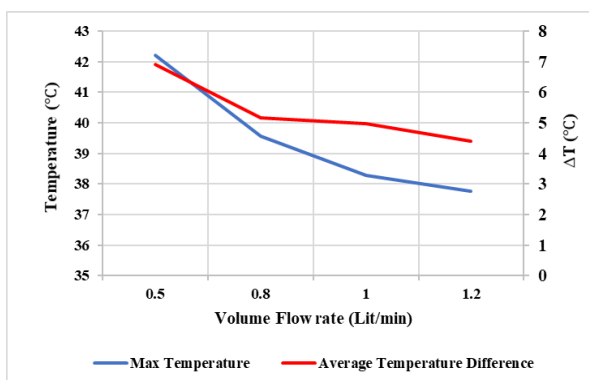

Figure 13: Effect of the volume flow rate on maximum temperature and average temperature difference of battery cells

According to Figure 13, the maximum temperature and temperature difference decreases when the coolant flow rate increases. Based on the permissible limit for the temperature difference between the battery cells, the minimum required coolant flow rate should be 1 Lit/min.
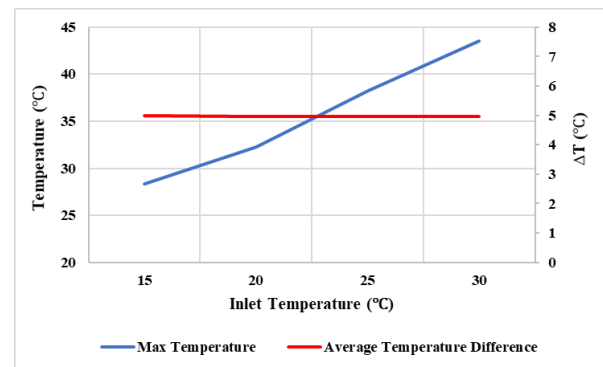

Figure 14: Effect of inlet coolant temperature on maximum temperature and average temperature difference of battery cells

As seen in Figure 14, the maximum temperature of battery cells rises when the inlet coolant temperature increases. However, increasing the inlet coolant temperature does not affect the temperature difference across the pack.

4. Conclusions

In this research, we investigated the impact of inlet coolant temperature and volume flow rate on the thermal behavior of the battery pack. The results of the numerical simulation are summarized as follows:

- Increasing the inlet temperature from 15 °C to 30 °C can increase the maximum temperature of the battery pack by 35%.

- The minimum flow rate of 1 Lit/min could keep the temperature difference within the battery pack lower than 5 °C.

- Increasing the volume flow rate from 0.5 to 1.2 Lit/min can reduce the maximum temperature and average temperature difference by 36% and 11%. However, the higher flow rate leads to a pressure drop increment.

Declaration of Conflicting Interests

The authors declared no potential conflicts of interest for the research, authorship, and/or publication of this article.

Acknowledgments

List of symbols

P	Pressure
u	Velocity
T	Temperature
K	Thermal Conductivity
C_p	Specific heat

Greek symbols

ρ	Density
μ	Dynamic viscosity

References

[1] Y. Li, H. Guo, F. Qi, Z. Guo, M. Li, L.B.J.A.T.E. Tjernberg. Investigation on liquid cold plate thermal management system with heat pipes for LiFePO4 battery pack in electric vehicles. Applied Thermal Engineering. 185 (2021) 116382.

[2] L. Liang, Y. Zhao, Y. Diao, R. Ren, H.J.E. Jing. Inclined U-shaped flat microheat pipe array configuration for cooling and heating lithium-ion battery modules in electric vehicles. Energy. 235 (2021) 121433.

[3] D. Huang, Z. Chen, S.J.E. Zhou. Model prediction-based battery-powered heating method for series-connected lithium-ion battery pack working at extremely cold temperatures. Energy. 216 (2021) 119236.

[4] J. Zhang, X. Wu, K. Chen, D. Zhou, M.J.J.o.P.S. Song. Experimental and numerical studies on an efficient transient heat transfer model for air-cooled battery thermal management systems. Journal of Power Sources. 490 (2021) 229539.

[5] L. Zhang, W. Fan, Z. Wang, W. Li, D.U.J.J.o.E.S. Sauer. Battery heating for lithium-ion batteries based on multi-stage alternative currents. Journal of Energy Storage. 32 (2020) 101885.

[6] X. Hu, Y. Zheng, D.A. Howey, H. Perez, A. Foley, M.J.P.i.E. Pecht, et al. Battery warm-up methodologies at subzero temperatures for automotive applications: Recent advances and perspectives. Progress in Energy Combustion Science 77 (2020) 100806.

[7] W. Wu, S. Wang, W. Wu, K. Chen, S. Hong, Y.J.E.c. Lai, et al. A critical review of battery thermal performance and liquid based battery thermal management. Energy conversion management.182 (2019) 262-81.

[8] J. Kim, J. Oh, H.J.A.t.e. Lee. Review on battery thermal management system for electric vehicles. Applied thermal engineering. 149 (2019) 192-212.

[9] J. Lin, X. Liu, S. Li, C. Zhang, S.J.I.J.o.H. Yang, M. Transfer. A review on recent progress, challenges and perspective of battery thermal management system. International Journal of Heat Mass Transfer. 167 (2021) 120834.

[10] P.R. Tete, M.M. Gupta, S.S.J.J.o.E.S. Joshi. Developments in battery thermal management systems for electric vehicles: A technical review. Journal of Energy Storage. 35 (2021) 102255.

[11] Q. Yue, C. He, H. Jiang, M. Wu, T.J.I.J.o.H. Zhao, M. Transfer. A hybrid battery thermal management system for electric vehicles under dynamic working conditions. International Journal of Heat Mass Transfer. 164 (2021) 120528.

[12] Z. Tang, X. Min, A. Song, J.J.J.o.E.E. Cheng. Thermal management of a cylindrical lithium-ion battery module using a multichannel wavy tube. Journal of Energy Engineering. 145 (2019) 04018072.

[13] G. Xia, L. Cao, G.J.J.o.p.s. Bi. A review on battery thermal management in electric vehicle application. Journal of power sources. 367 (2017) 90-105.

[14] J. Jaguemont, L. Boulon, Y.J.A.E. Dubé. A comprehensive review of lithium-ion batteries used in hybrid and electric vehicles at cold temperatures. Applied Energy. 164 (2016) 99-114.

[15] A.A.J.J.o.p.s. Pesaran. Battery thermal models for hybrid vehicle simulations. 110 (2002) 377-82.

[16] M.R. Giuliano, A.K. Prasad, S.G.J.J.o.p.s. Advani. Experimental study of an air-cooled thermal management system for high capacity lithium–titanate batteries. Journal of power sources. 216 (2012) 345-52.

[17] E.W. Lemmon, R.T.J.I.j.o.t. Jacobsen. Viscosity and thermal conductivity equations for nitrogen, oxygen, argon, and air. International journal of thermophysics. 25 (2004) 21-69.

[18] M.R. Giuliano, S.G. Advani, A.K.J.J.o.P.S. Prasad. Thermal analysis and management of lithium–titanate batteries. J Journal of Power Sources. 196 (2011) 6517-24.

[19] R. Jilte, R. Kumar, M.H.J.J.o.C.P. Ahmadi. Cooling performance of nanofluid submerged vs. nanofluid circulated battery thermal management systems. Journal of Cleaner Production. 240 (2019) 118131.

[20] L. Jin, P. Lee, X. Kong, Y. Fan, S.J.A.e. Chou. Ultra-thin minichannel LCP for EV battery thermal management. Applied energy. 113 (2014) 1786-94.

[21] S. Panchal, I. Dincer, M. Agelin-Chaab, R. Fraser, M.J.A.T.E. Fowler. Thermal modeling and validation of temperature distributions in a prismatic lithium-ion battery at different discharge rates and varying boundary conditions. Applied Thermal Engineering. 96 (2016) 190-9.

[22] S. Panchal, K. Gudlanarva, M.-K. Tran, R. Fraser, M.J.E. Fowler. High reynold's number turbulent model for micro-channel cold plate using reverse engineering approach for water-cooled battery in electric vehicles. Energies. 13 (2020) 1638.

[23] A. Pruteanu, B.V. Florean, G.M. Moraru, R.C. Ciobanu. Development of a thermal simulation and testing model for a superior lithium-ion-polymer battery. 2012 13th International Conference on Optimization of Electrical and Electronic Equipment (OPTIM). IEEE2012. pp. 947-52.

[24] J. Yi, U.S. Kim, C.B. Shin, T. Han, S.J.J.o.t.E.S. Park. Three-dimensional thermal modeling of a lithium-ion battery considering the combined effects of the electrical and thermal contact resistances between current collecting tab and lead wire. Journal of the Electrochemical Society. 160 (2013) A437.

[25] C.J.I.T.o.V.T. Alaoui. Solid-state thermal management for lithium-ion EV batteries. IEEE Transactions on Vehicular Technology. 62 (2012) 98-107.

[26] A. Smyshlyaev, M. Krstic, N. Chaturvedi, J. Ahmed, A. Kojic. PDE model for thermal dynamics of a large Li-ion battery pack. Proceedings of the 2011 American Control Conference. IEEE2011. pp. 959-64.

[27] Z. Wang, W. Fan, P.J.E.P. Liu. Simulation of temperature field of lithium battery pack based on computational fluid dynamics. Energy Procedia. 105 (2017) 3339-44.

[28] G. Li, S.J.E.T. Li. Physics-based CFD simulation of lithium-ion battery under the FUDS driving cycle. ECS Transactions. 64 (2015).

[29] H. Behi, D. Karimi, M. Behi, M. Ghanbarpour, J. Jaguemont, M.A. Sokkeh, et al. A new concept of thermal management system in Li-ion battery using air cooling and heat pipe for electric vehicles. Applied Thermal Engineering. 174 (2020) 115280.

[30] C. Lin, S. Xu, G. Chang, J.J.J.o.P.S. Liu. Experiment and simulation of a LiFePO4 battery pack with a passive thermal management system using composite phase change material and graphite sheets. Journal of Power Sources. 275 (2015) 742-9.

[31] Z. Rao, Q. Wang, C.J.A.e. Huang. Investigation of the thermal performance of phase change material/mini-channel coupled battery thermal management system. Applied energy. 164 (2016) 659-69.

[32] A. Mir Mohammadi, M.R. Kolki. The 11th International Conference On Internal Combustion Engine and Oil. (2019).(In Persian)

[33] T. Wang, K. Tseng, J. Zhao, Z.J.A.e. Wei. Thermal investigation of lithium-ion battery module with different cell arrangement structures and forced air-cooling strategies. Applied energy. 134 (2014) 229-38.

[34] S. Wang, K. Li, Y. Tian, J. Wang, Y. Wu, S.J.A.T.E. Ji. Improved thermal performance of a large laminated lithium-ion power battery by reciprocating air flow. Applied Thermal Engineering. 152 (2019) 445-54.

[35] Y. Huo, Z. Rao, X. Liu, J.J.E.C. Zhao, Management. Investigation of power battery thermal management by using mini-channel cold plate. Energy Conversion Management. 89 (2015) 387-95.

[36]https://www.ansys.com/products/fluids/ansys-fluent/mosaic meshing.

[37] L.H. Saw, Y. Ye, A.A. Tay, W.T. Chong, S.H. Kuan, M.C.J.A.e. Yew. Computational fluid dynamic and thermal analysis of Lithium-ion battery pack with air cooling. Applied Energy. 177 (2016) 783-92.

[38] T. Kang, S. Park, P.-Y. Lee, I.-H. Cho, K. Yoo, J.J.E. Kim. Thermal Analysis of a Parallel-Configured Battery Pack (1S18P) Using 21700 Cells for a Battery-Powered Train. Electronics. 9 (2020) 447.